Cerebellar Expression of Copper Chaperone for Superoxide, Cytosolic Cu/Zn-Superoxide Dismutase, 4-Hydroxy-2-Nonenal, Acrolein and Heat Shock Protein 32 in Patients with Menkes Kinky Hair Disease: Immunohistochemical Study

Atsushi Yokoyama,*† Kousaku Ohno,†‡ Asao Hirano,§ Masayuki Shintaku,‖ Masako Kato,¶ Kazuhiko Hayashi¶ and Shinsuke Kato*

**Division of Neuropathology, Department of Pathology, School of Medicine, Tottori University Faculty of Medicine, Yonago, 683-8503, Japan, †Division of Child Neurology, Department of Brain and Neurosciences, School of Medicine, Tottori University Faculty of Medicine, Yonago, 683-8503, Japan, ‡Sanin Rosai Hospital, Yonago, 683-8605, Japan, §Division of Neuropathology, Department of Pathology, Montefiore Medical Center, Albert Einstein College of Medicine, Bronx, NY 10461, United States, ‖Department of Pathology, Osaka Red Cross Hospital, Osaka 543-8555, Japan and ¶Division of Molecular Pathology, Department of Pathology, School of Medicine, Tottori University Faculty of Medicine, Yonago, 683-8503, Japan*

ABSTRACT

Background To clarify the pathogenesis of cerebellar Purkinje cell death in patients with Menkes kinky hair disease (MD), a disorder of copper absorption, we investigated the morphological and functional abnormalities of residual Purkinje cells in MD patients and the mechanism of cell death.

Methods Seven MD patients and 39 neurologically normal autopsy cases were studied. We performed histopathological and quantitative analyses of the Purkinje cells. In addition, we used immunohistochemistry to detect copper-dependent enzymes [cytosolic Cu/Zn-superoxide dismutase (SOD1) and copper chaperone for superoxide dismutase (CCS)], oxidative stress markers [4-hydroxy-2-nonenal (HNE) and acrolein] and heat shock protein (hsp) 32.

Results The surviving MD Purkinje cells showed abnormal development, such as somatic sprouts and heterotopic location. Due to maldevelopment and degeneration, dendrites showed the cactus and weeping willow patterns. Axonal degeneration led to the formation of torpedoes. Quantitative analysis revealed loss of approximately 50% of the Purkinje cells in MD patients. Almost all of the normal Purkinje cells were positive for immunostaining by anti-CCS and anti-SOD1 antibodies, with staining of the cell bodies, dendrites and axons. Normal Purkinje cells were not stained by antibodies for HNE, acrolein or hsp 32. In MD patients, the majority of Purkinje cells were positive for CCS, but the positive rate for SOD1 was only about 23%. Approximately 56%, 42% and 40% of the Purkinje cells of MD patients were positive for HNE, acrolein and hsp 32, respectively.

Conclusion In MD patients, about 50% of the Purkinje cells have been lost due to maldevelopment and degeneration. In the residual Purkinje cells, CCS expression seems to be nearly normal as a protective response to decreased SOD1 activity due to copper deficiency. Because oxidative stress is elevated secondary to decreased SOD1 activity, hsp 32 is induced as another protective mechanism.

Key words copper chaperone for superoxide dismutase; cytosolic Cu/Zn-superoxide dismutase; immunohistochemistry; Menkes kinky hair disease; Purkinje cell

Menkes kinky hair disease (MD) is a sex-linked inherited disorder that is characterized by the onset of seizures, developmental retardation and typical changes of the hair in early infancy.[1–5] MD patients develop neuropathological abnormalities throughout the central nervous system.[4–7] In the cerebellar cortex, there is marked loss of Purkinje cells, while the surviving Purkinje cells display characteristic somatic sprouts and bizarre thickening of the dendritic tree.[4, 5, 8–10] Several studies have shown that severe hypocuprinemia occurs in MD patients due to impaired absorption of copper from the intestine, which causes inactivation of copper-dependent enzymes such as cytosolic Cu/Zn-binding superoxide dismutase (SOD1).[11]

SOD1 is usually a dimer of 2 identical monomers with a molecular weight of approximately 16 kDa, and is mainly localized to the cytoplasm. Each SOD1 monomer contains one Cu ion and one Zn ion. SOD1 is an antioxidant metalloenzyme that catalyzes the conversion of 2 superoxide radicals ($O_2^{\bullet-}$) to 1 molecule each of

Corresponding author: Shinsuke Kato, MD, PhD
kato@med.tottori-u.ac.jp
Received 2013 November 8
Accepted 2013 November 19

Abbreviations: ABC, avidin-biotin-immunoperoxidase complex; ANOVA, analysis of variance; BSA-PBS, phosphate-buffered saline with 1% bovine serum albumin; CCS, copper chaperone for superoxide dismutase; HE, hematoxylin and eosin; HNE, 4-hydroxy-2-nonenal; MD, Menkes kinky hair disease; SOD1, cytosolic Cu/Zn-superoxide dismutase; hsp, heat shock protein

H_2O_2 and O_2.[12, 13] An $O_2^{\bullet-}$ is formed when an oxygen molecule accepts an additional electron. Superoxide radicals cause oxidative damage to the nuclei, organelles and enzymes of cells, by reacting with nucleic acids in the nuclei, proteins that compose cytoplasmic organelles and proteins of enzymes, respectively. Under normal conditions, the copper ion of SOD1 exists in the divalent state. When this Cu^{2+} of SOD1 reacts with an $O_2^{\bullet-}$, it undergoes reduction to a Cu^{+} by gaining an electron from the superoxide radical, while the radical that reacted with the Cu^{2+} of SOD1 is converted to O_2. Then the Cu^{+} of SOD1 is oxidized again to return to its original divalent state as it supplies an electron to another $O_2^{\bullet-}$. This other $O_2^{\bullet-}$ that receives an electron from the Cu^{+} of SOD1 is converted to H_2O_2 by reacting with $2H^{+}$. Thus, SOD1 catalyzes the conversion of 2 $O_2^{\bullet-}$ to 1 molecule of H_2O_2 and 1 molecule of O_2.[12, 13] The H_2O_2 generated by this reaction is ultimately transformed into H_2O and O_2 by enzymes such as catalase, glutathione peroxidase and peroxiredoxin.[13–15]

The yeast copper chaperone (LSY7: 249 amino acids) and the mammalian copper chaperone for superoxide dismutase (CCS: 274 amino acids) have both been identified.[16] The RNA for CCS is encoded by a single-copy gene on chromosome 11, and CCS expression has been found in all human tissues and cells examined.[16, 17] CCS specifically transfers copper ions to SOD1, resulting in its activation.[16, 18] Since there are no free copper ions in vivo,[19] SOD1 cannot obtain copper without CCS and cannot be activated, so the delivery of copper to SOD1 by CCS is essential for its normal activity.[20]

Extracellular copper ions are transported into the cytoplasm by copper transporter 1 located in the cell membrane.[21, 22] CCS has 3 domains, among which domain I contains a copper-binding site for the copper ions that it transports. Copper ions that bind to domain I are transferred to domain III via domain II. Domain II of CCS shows structural similarity to SOD1 at the molecular level and contains the coupling region for binding with SOD1. After the copper ion is transferred from the copper-binding site on domain I to the copper-binding site on domain III, it is supplied to SOD1.

Therefore, CCS has an important, though indirect, role in fighting oxidative stresses. Immunohistochemical studies have shown that CCS is extensively distributed throughout the normal central nervous system, including the cerebellar Purkinje cells, similar to SOD1.[17] Decreased SOD1 activity due to impaired absorption of copper could cause cellular damage in MD patients, with oxidative stress leading to oxidation of membrane lipids and the production of toxic aldehyde metabolites such as 4-hydroxy-2-nonenal (HNE) or acrolein. Furthermore, heat shock protein (hsp) 32 would be induced in response to the increase of oxidative stress.

In MD patients, copper deficiency could be expected to lead to Purkinje cell damage due to oxidative stress. In the present study, we performed an immunohistochemical analysis of cerebellar CCS and SOD1 as copper-dependent enzymes, HNE and acrolein as markers of oxidative stress and hsp 32 as a stress protein. We also carried out a quantitative analysis of the number of Purkinje cells in the cerebellum. Our objectives were to clarify the morphological and functional abnormalities of Purkinje cells in MD patients and the pathogenesis of these Purkinje cell changes.

MATERIALS AND METHODS

Subjects and neuropathologic examination

This study was carried out on brain tissues obtained at autopsy from 7 patients with Menkes kinky hair disease (MD). The main characteristics of these 7 patients are summarized in Table 1. Histologically normal brains from 39 other autopsy patients (ages: 1–59 years) served as the controls. After fixation in 10% buffered formalin, the brain stem and cerebellum were removed from the cerebrum at the midbrain level. Routine coronal slices of the cerebrum and sagittal and transverse slices of the cerebellum were cut. The thickness of these slices was about 5 mm and each slice completely transected the cerebrum and cerebellum. Slices of the cerebellum were embedded in paraffin and then were cut into 6-μm thick sections, which were stained by using the following routine methods: hematoxylin and eosin (HE), Klüver-Barrera, Holzer, Bodian and modified Hirano-Bielschowsky stains. Representative paraffin sections were used for the immunohistochemical analyses. The protocol of this study was approved by the Ethics Committee of Tottori University (No. 1994: 2012).

Quantitative analysis of cerebellar Purkinje cells

We performed quantitative analysis of the number of Purkinje cells in the cerebellum using HE-stained sagittal and transverse sections of the cerebellar hemisphere and vermis on glass slides (Fig. 1A). The number of Purkinje cells was counted within a 3 mm length, as shown in Fig. 1B. For determining the 3 mm length of the circle in Fig. 1A, we used a light microscope (Olympus BX-50 F4, Tokyo, Japan) equipped with an eyepiece micrometer grid (24-#10/10X10, Olympus), in combination with the stage micrometer (AX0001, OB-M, Olympus). To determine the number of Purkinje cells, we counted the number of these cells with nuclei. As shown in Fig. 1B, we counted the number of Purkinje cells within this 3 mm length using a measuring device (Erma, Tokyo,

Table 1. Characteristics of the 7 patients with Menkes kinky hair disease

	Patient 1	Patient 2	Patient 3	Patient 4	Patient 5	Patient 6	Patient 7
Age at death	1 yr 1 mo	1 yr 4 mo	1 yr 6 mo	1 yr 6 mo	1 yr 9 mo	2 yr 1 mo	6 yr 4 mo
Brain weight (g)	650	500	700	580	450	720	1,130
Family history	–	–	–	+*	+	+*	?
Reference number	4, 5, 36, 37	4, 5	4, 5, 36, 37	4, 5, 36, 37	4, 5, 36, 37	4, 5, 36, 37	4, 5, 38

*sibling; –, absent; +, present; ?, unknown.

Japan). In each autopsy case, these circles including the 3 mm length (Fig. 1A) were selected randomly at 15 to 80 sites on HE-stained sections of the cerebellar hemisphere and vermis on glass slides. Then we determined the mean number of Purkinje cells per 3 mm length for each autopsy case.

Immunohistochemistry

The following primary antibodies were used: an affinity purified rabbit antibody directed against human copper chaperone for superoxide dismutase (CCS) [diluted 1:500 in phosphate-buffered saline with 1% bovine serum albumin (BSA-PBS), pH 7.4],[23, 24] a rabbit polyclonal antibody for human SOD1 (diluted 1:3,000),[12, 14, 15, 23, 25–29] an affinity purified rabbit antibody targeting 4-hydroxy-2-nonenal (HNE) (diluted 1:400; JaICA, Fukuroi, Japan), a rabbit polyclonal antibody for acrolein (diluted 1:3,000; JaICA) and a rabbit polyclonal antibody directed against hsp 32 (diluted 1:200; Santa Cruz, Dallas, TX). The specificity of these antibodies for immunohistochemical detection of the respective epitopes in paraffin sections of human materials has been documented previously.[12, 14, 15, 23–29]

Sections were deparaffinized, and endogenous peroxidase activity was quenched by incubation for 30 min with 0.3% H_2O_2. Then the sections were washed in PBS (pH 7.4). Normal serum homologous to each secondary antibody was used as the blocking agent. Sections were incubated with the primary antibodies for 18 h at 4 ˚C and sections incubated with PBS served as controls. Bound antibodies were visualized by the avidin-biotin-immunoperoxidase complex (ABC) method using the appropriate Vectorstain ABC kit (Vector Laboratories, Burlingame, CA) and 3,3′-diaminobenzidine tetrahydrochloride (Dako, Glostrup, Denmark).

The cellular structures on immunostained sections were observed under a light microscope (Olympus BX-50 F4) and mapped, and photomicrographs were obtained using a digital camera (Olympus DP12). Then representative immunostained sections were also subjected to HE staining.

To assess immunostaining of the Purkinje cells in the cerebellum by each antibody, 1,000 Purkinje cells were examined. Cells that were immunoreactive to the respective primary antibodies were considered to be positive and the proportion of antibody-positive cells was expressed as a percentage.

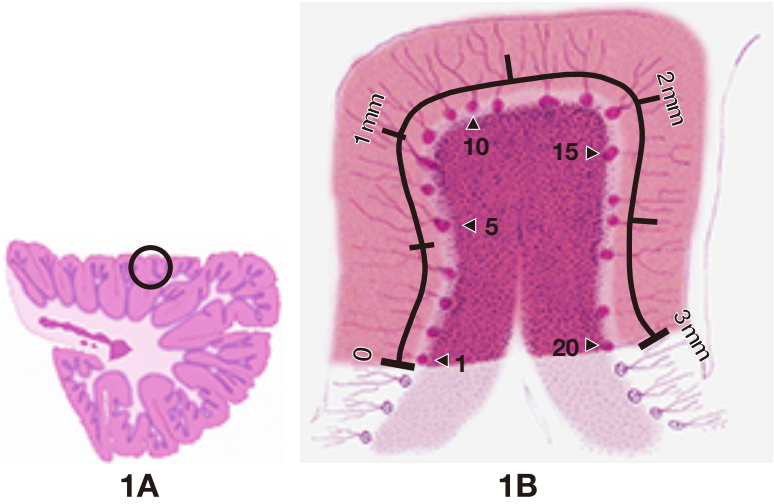

Fig. 1. Diagram of the method for quantitative measurement of the number of Purkinje cells in the cerebellum.

A: Sagittal section of the cerebellar hemisphere. The circle shown in **A** involves a 3 mm length of the Purkinje cell layer. The circled area was used for quantitative determination of the number of Purkinje cells. In each autopsy case, at least 15 sites were randomly selected from a sagittal section of the cerebellar hemisphere, and the number of Purkinje cells was counted in each area.

B: An enlarged image of the circle shown in **A**. We measure a 3 mm length (indicated by 3 mm in **B**) in the cerebellar Purkinje cell layer and count the number of red-stained Purkinje cells within this 3 mm length. For example, there are 20 Purkinje cells in **B**.

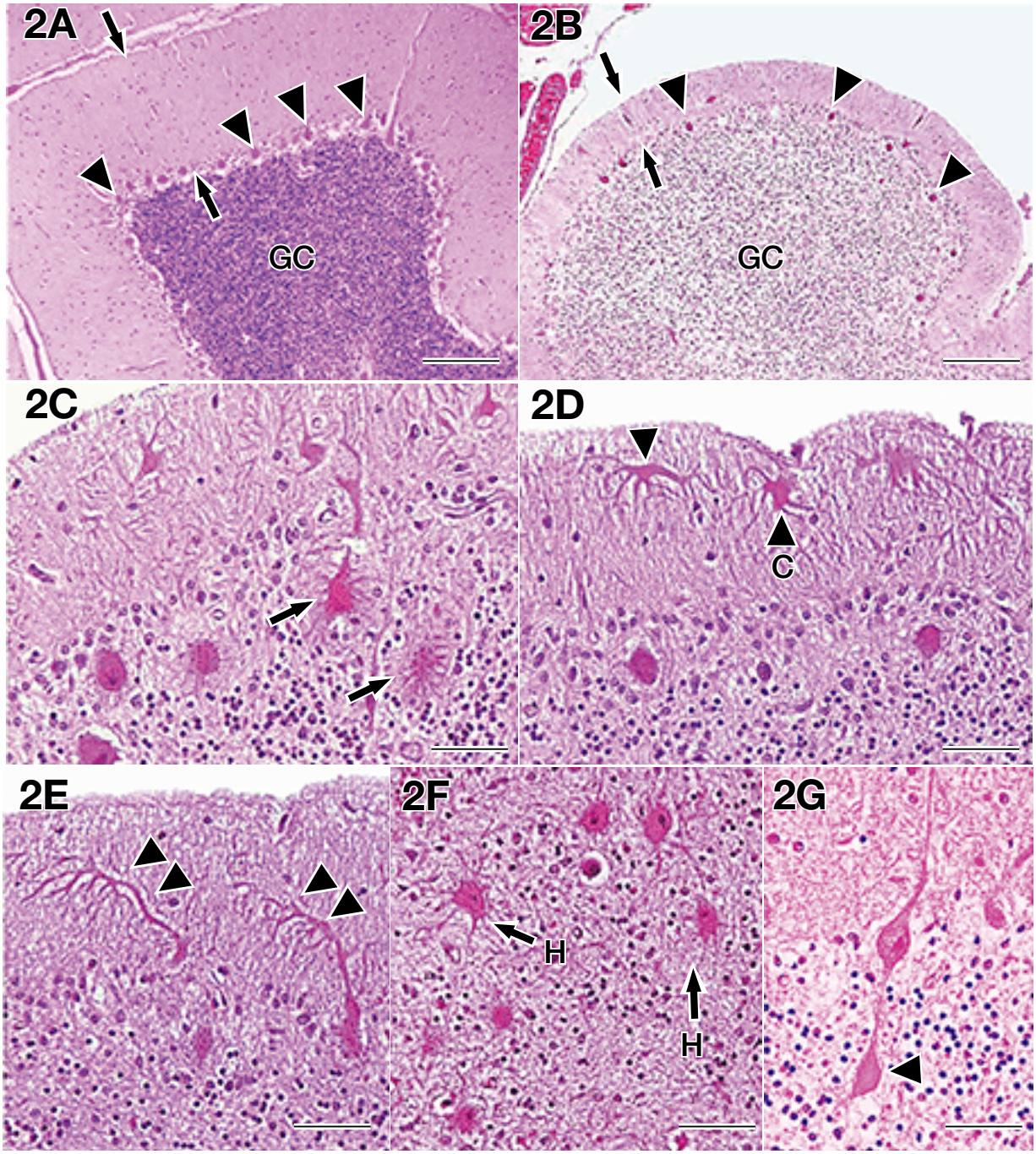

Fig. 2. Histologic features of Purkinje cells in a normal control autopsy case (**A**) and an MD patient (**B**–**G**).

A: Cerebellum of a normal control autopsy case.

B: Cerebellum of an MD patient. Compared with the normal cerebellum, the cerebellum of the MD patient shows severe loss of Purkinje cells (arrowheads in **A** and **B**) and marked reduction of granule cells (GC in **A** and **B**). As a result, there is a marked decrease in the width of the molecular cell layer (arrows in **A** and **B**). Panels **A** and **B** are at the same magnification (HE stain). Bars = 200 μm (**A** and **B**).

C: The residual Purkinje cells of the MD patient show somatic sprouts (arrows) (HE stain). Bar = 50 μm.

D: Surviving Purkinje cells of the MD patient exhibit cactus-like change (arrowhead and **C**) and dendritic expansion (arrowhead) (HE stain). Bar = 50 μm.

E: Residual Purkinje cells of the MD patient display a weeping willow dendritic pattern (double arrowheads) (HE stain). Bar = 50 μm.

F: In the MD patient, ectopic Purkinje cells bearing somatic sprouts (arrows and **H**) are found in the granule cell layer (HE stain). Bar = 50 μm.

G: A residual Purkinje cell of the MD patient shows an axonal torpedo (arrowhead) (HE stain). Bar = 50 μm.

HE, hematoxylin and eosin; MD, Menkes kinky hair disease.

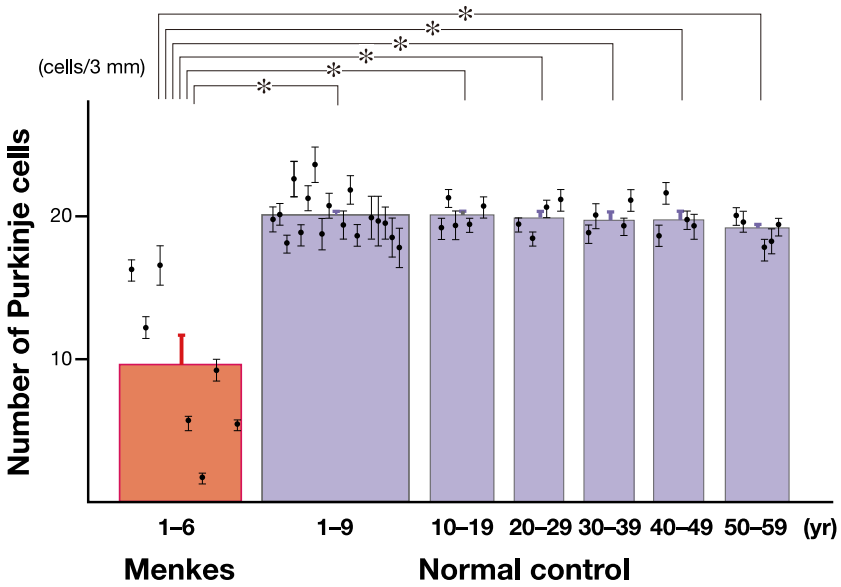

Fig. 3. Quantitative analysis of the number of Purkinje cells in the cerebellum. The number of Purkinje cells in each autopsy case is shown as mean ± SE. Compared with the number of Purkinje cells in the normal controls, the number of Purkinje cells was significantly low in the MD patients. Error bars represent SE. *$P < 0.01$ compared with the normal control autopsy cases by Kruskal-Wallis analysis of variance, followed by the Wilcoxon rank-sum test.

Statistical analysis

IBM SPSS Statistics software (IBM, Chicago, IL) was used for statistical analysis. The number of Purkinje cells is presented as the mean ± SE. For analysis of all data, non-parametric Kruskal-Wallis analysis of variance (ANOVA) was performed, followed by a non-parametric Wilcoxon rank-sum test. Statistical significance was accepted at $P < 0.05$.

RESULTS

Neuropathological findings

Comparison between the 39 normal control autopsy cases (Fig. 2A) and the 7 MD autopsy cases (Fig. 2B) revealed severe loss of Purkinje cells and marked reduction of granule cells (Fig. 2B) in the cerebellum of the MD patients. The loss of Purkinje cells in MD patients was accompanied by prominent Bergmann gliosis in the Purkinje cell layer. In all 7 MD patients, the width of the molecular layer of the cerebellum, which is mainly composed of Purkinje cell dendrites and the parallel fiber axons of granule cells, was significantly decreased (Fig. 2B) in comparison with that of the control autopsy cases, reflecting the marked loss of Purkinje cells and granule cells in the MD patients.

The chief neuropathological characteristic in the cytoplasm of the residual Purkinje cells of MD patients was somatic sprouts (Fig. 2C). The neuropathological abnormalities of the dendrites of the residual Purkinje cells in MD patients included expansion and cactus-like changes, i. e., partial enlargement of Purkinje cell dendrites was observed (Fig. 2D). With respect to abnormal dendritic arborization in the residual Purkinje cells, we observed downward extension of the dendrites, which has been called the weeping willow pattern by Kato et al.[5] (Fig. 2E). In the granule cell layer of MD patients, the presence of heterotopic Purkinje cells bearing somatic sprouts was noted (Fig. 2F). In addition, the residual Purkinje cells of MD patients displayed axonal expansions that are known as torpedoes (Fig. 2G).

Quantitative analysis of Purkinje cell changes

The mean number (± SE) of residual Purkinje cells in all 7 MD autopsy cases was 9.1 ± 2.1 cells/3 mm. In contrast, the mean number (± SE) of Purkinje cells in the normal cerebellum at the age of 1 to 9 years, 10 to 19 years, 20 to 29 years, 30 to 39 years, 40 to 49 years and 50 to 59 years was 20.1 ± 0.4 cells/3 mm, 20.1 ± 0.4 cells/3 mm, 20.0 ± 0.6 cells/3 mm, 19.9 ± 0.5 cells/3 mm, 19.9 ± 0.6 cells/3 mm and 19.2 ± 0.4 cells/3 mm, respectively (Fig. 3). There was a significant decrease of Purkinje cells in the MD patients compared with the number of cells in the controls ($P < 0.01$, Kruskal-Wallis test with ANOVA). We also performed a comparison between the number of residual Purkinje cells in MD patients and the number of Purkinje cells in normal children from the age of 1 to 9 years. As a result, there was a significant decrease in the number of Purkinje cells in the MD patients ($P < 0.01$, Wilcoxon rank-sum test). Furthermore, we performed between-group analyses to compare the number of residual Purkinje cells in the

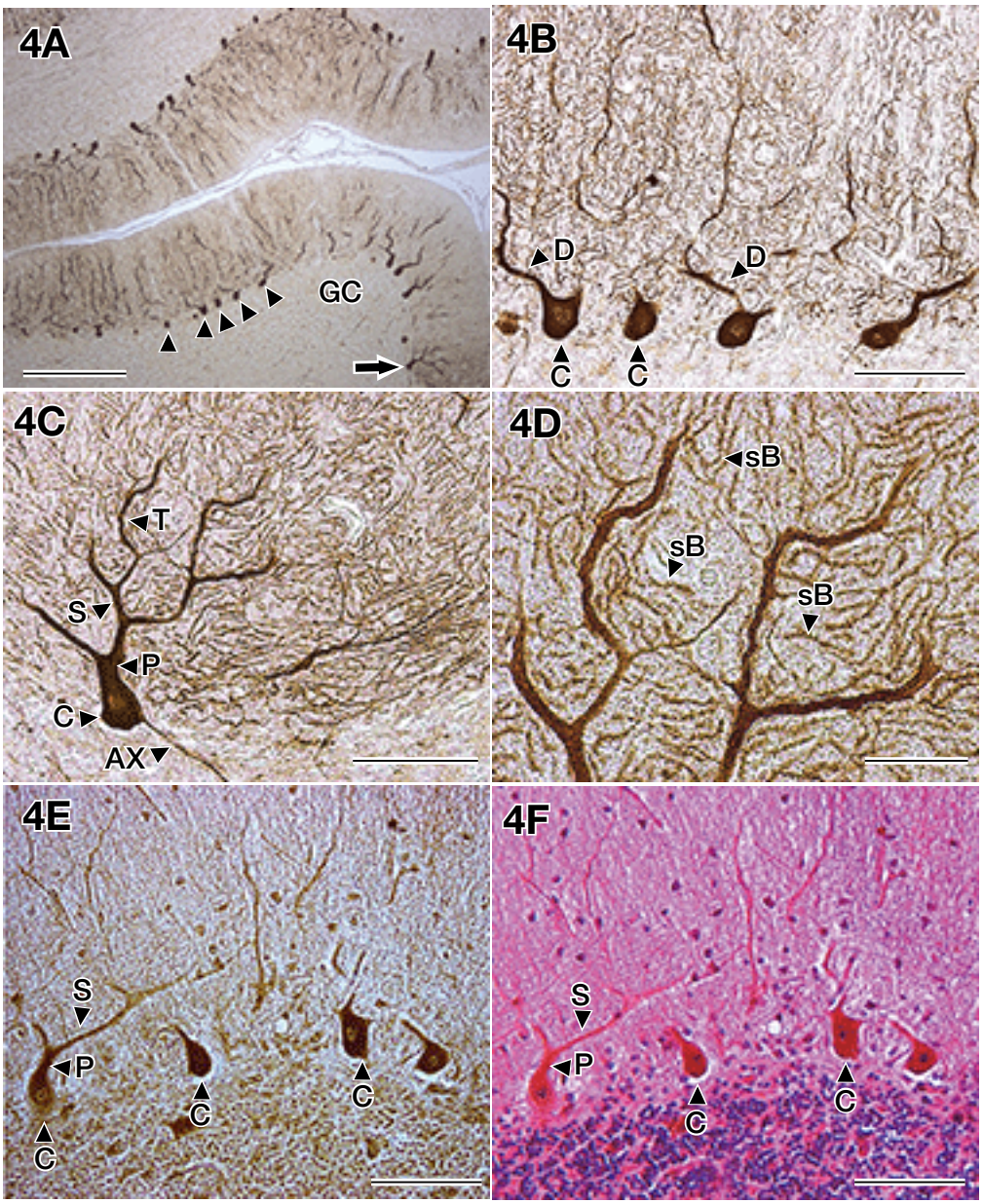

Fig. 4. Immunohistochemical expression of CCS (**A**–**D**) and SOD1 (**E**) by the Purkinje cells of a normal control.

A: Almost all of the Purkinje cells in the normal cerebellum are stained by the antibody for CCS (arrowheads and arrow), while granule cells (GC) do not react with the anti-CCS antibody (CCS immunostaining without counterstaining). Bar = 500 µm.

B: Higher magnification of the Purkinje cells identified by arrowheads in **A**. The cell bodies (arrowheads with C) and dendrites (arrowheads with D) are readily seen (CCS immunostaining without counterstaining). Bar = 100 µm.

C: Higher magnification of the Purkinje cells indicated by an arrow in **A**. The cell body (arrowhead with C), primary dendrites (arrowhead with P), secondary dendrites (arrowhead with S) and tertiary dendrites (arrowhead with T), as well as an axon (arrowhead with AX), are clearly seen (CCS immunostaining without counterstaining). Bar = 100 µm.

D: High-powered view of the Purkinje cell dendrites indicated by the arrowhead with S and arrowhead with T in **C**. Many spiny branchlets (arrowhead with sB) are clearly observed (CCS immunostaining without counterstaining). Bar = 30 µm.

E and **F:** Preparations of the same section of normal control cerebellar cortex stained with anti-SOD1 antibody (**E**) or with HE (**F**). Almost all of the Purkinje cells in the normal control cerebellum are stained by the anti-SOD1 antibody with varying intensity. Purkinje cell bodies (arrowheads with C) are positive, as are their main dendrites, including the primary dendrites (arrowhead with P) and secondary dendrites (arrowhead with S) (**E:** SOD1 immunostaining without counterstaining. **F:** HE staining). Bars = 100 µm.

CCS, copper chaperone for superoxide dismutase; HE, hematoxylin and eosin; SOD1, cytosolic Cu/Zn-superoxide dismutase.

MD patients with the number of Purkinje cells in the normal control autopsy cases from age 10 to 19, from age 20 to 29, from age 30 to 39, from age 40 to 49 and from age 50 to 59 years. All of these analyses revealed

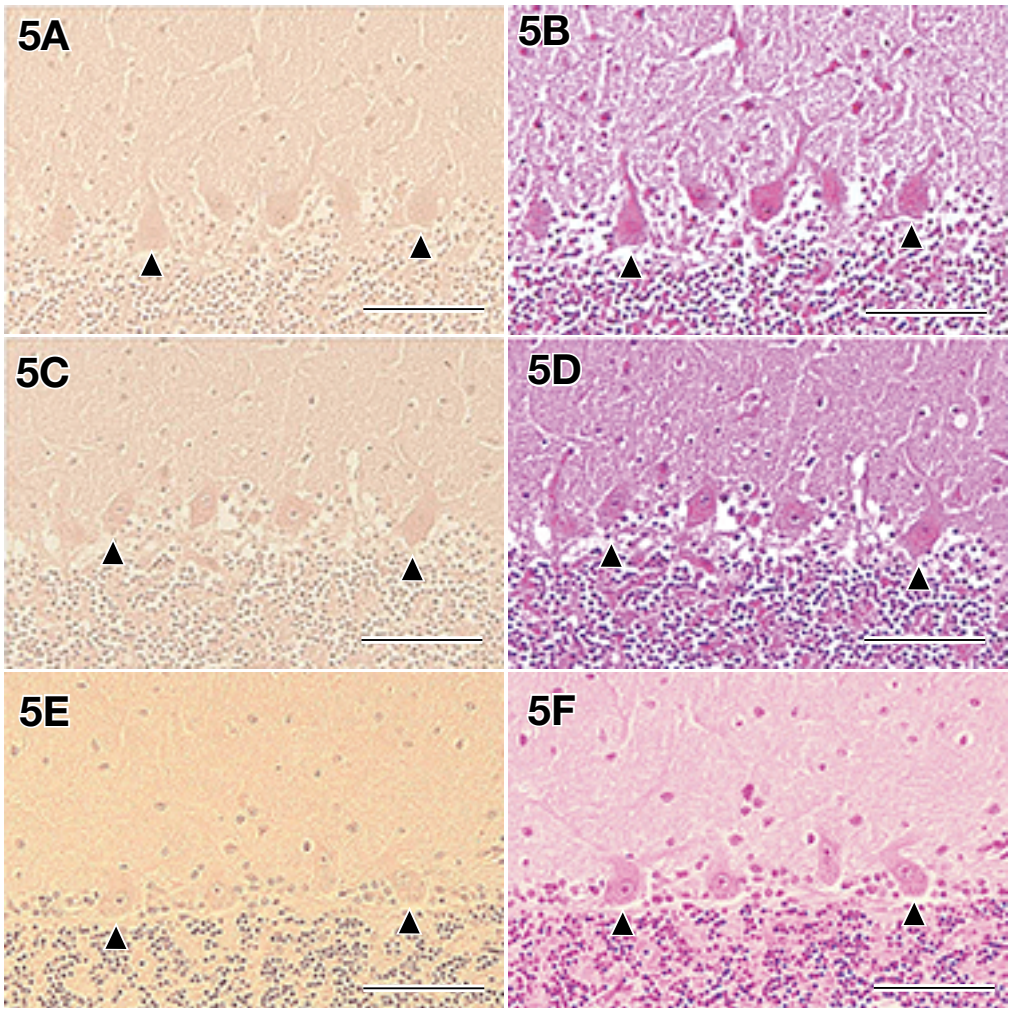

Fig. 5. Immunostaining of the cerebellum of a normal control with antibodies for HNE (**A**), acrolein (**C**) and hsp 32 (**E**). Normal Purkinje cells (arrowheads) are not stained by the antibodies for HNE (**A**), acrolein (**C**) and hsp 32 (**E**).
A: HNE immunostaining with weak hematoxylin counterstaining. Bar = 100 µm.
C: Acrolein immunostaining with weak hematoxylin counterstaining. Bar = 100 µm.
E: hsp32 immunostaining with weak hematoxylin counterstaining. Bar = 100 µm.
B, D, F: HE staining. Bars = 100 µm.
HE, hematoxylin and eosin; HNE, 4-hydroxy-2-nonenal; hsp, heat shock protein.

a significant decrease in the number of Purkinje cells in the MD patients ($P < 0.01$, Wilcoxon rank-sum test) (Fig. 3). In contrast, the number of Purkinje cells in the normal control autopsy cases showed no significant difference across the age groups from 1 to 59 years ($P > 0.2$, Kruskal-Wallis test with ANOVA).

Immunohistochemical findings

When control tissue sections were incubated with PBS, no immunoreaction products were seen. In the normal controls, Purkinje cells were stained by the antibody for CCS. Staining of the cell bodies, dendrites, and axons was seen, with the primary, secondary and tertiary dendrites as well as spiny branchlets being clearly detected (Figs. 4A–D). The axons could be traced to the dentate nucleus. The glial cells, myelin sheaths, blood vessels, leptomeninges and other neuronal cells of the normal cerebellum did not react with the anti-CCS antibody.

Purkinje cells of the normal cerebellum were also immunostained by the anti-SOD1 antibody, with the cell bodies and the main dendrites (including primary and secondary dendrites) being positive (Figs. 4E and F). Normal Purkinje cells did not show immunostaining by the antibodies for HNE (Fig. 5A), acrolein (Fig. 5C) or hsp 32 (Fig. 5E).

The surviving cerebellar Purkinje cells of MD patients differed from normal Purkinje cells in terms of both morphology and immunoreactivity. Residual Purkinje cells in MD patients showed immunostaining by the anti-CCS antibody at varying intensities and ap-

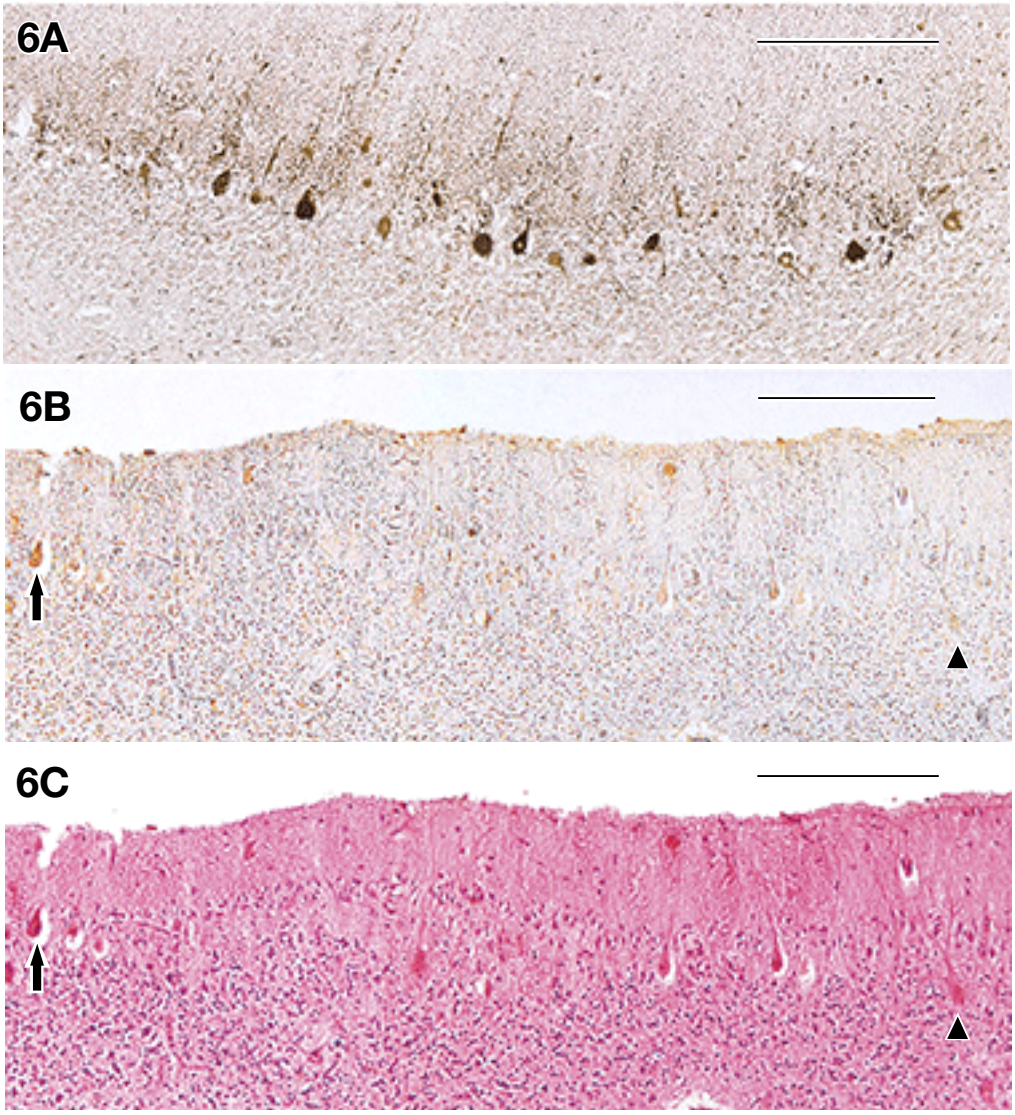

Fig. 6. Immunostaining of the cerebellum from a patient with MD using antibodies for CCS (**A**) and SOD1 (**B**).
A: Many of the surviving Purkinje cells are positive for CCS at varying intensities (CCS immunostaining without counterstaining). Bar = 200 µm.
B and **C**: Some of the surviving Purkinje cells (arrow in **B** and **C**) are positive for SOD1, while other cells (arrowhead in **B** and **C**) are negative (**B:** SOD1 immunostaining without counterstaining, **C:** HE staining). Bars = 200 µm.
CCS, copper chaperone for superoxide dismutase; HE, hematoxylin and eosin; MD, Menkes kinky hair disease; SOD1, cytosolic Cu/Zn-superoxide dismutase.

proximately 77% (773 ± 49.5/1,000) of these cells were positive for CCS (Fig. 6A). The most frequent immunostaining pattern was varying levels of CCS positivity in the cell bodies and the proximal parts of the dendrites of the Purkinje cells.

Immunostaining for SOD1 was positive in some of the surviving Purkinje cells of the MD patients, with the positive rate for anti-SOD1 antibody being about 23% (232 ± 89.0/1,000) but the staining intensity was low (Fig. 6B). When SOD1-positive and SOD1-negative Purkinje cells of the MD patients were compared by HE staining, it was impossible to clearly distinguish between them (Fig. 6C).

Immunostaining using anti-HNE antibody showed that many of the residual Purkinje cells were positive for HNE in MD patients. A variable staining intensity was observed (Fig. 7A), and the positive rate for anti-HNE antibody among the surviving Purkinje cells was approximately 56% (564 ± 55.8/1,000). When HNE-positive and HNE-negative Purkinje cells were compared by HE staining, it was not possible to observe any clear differences between them (Fig. 7B). Immunostaining with the anti-acrolein antibody demonstrated that some of the viable Purkinje cells in MD

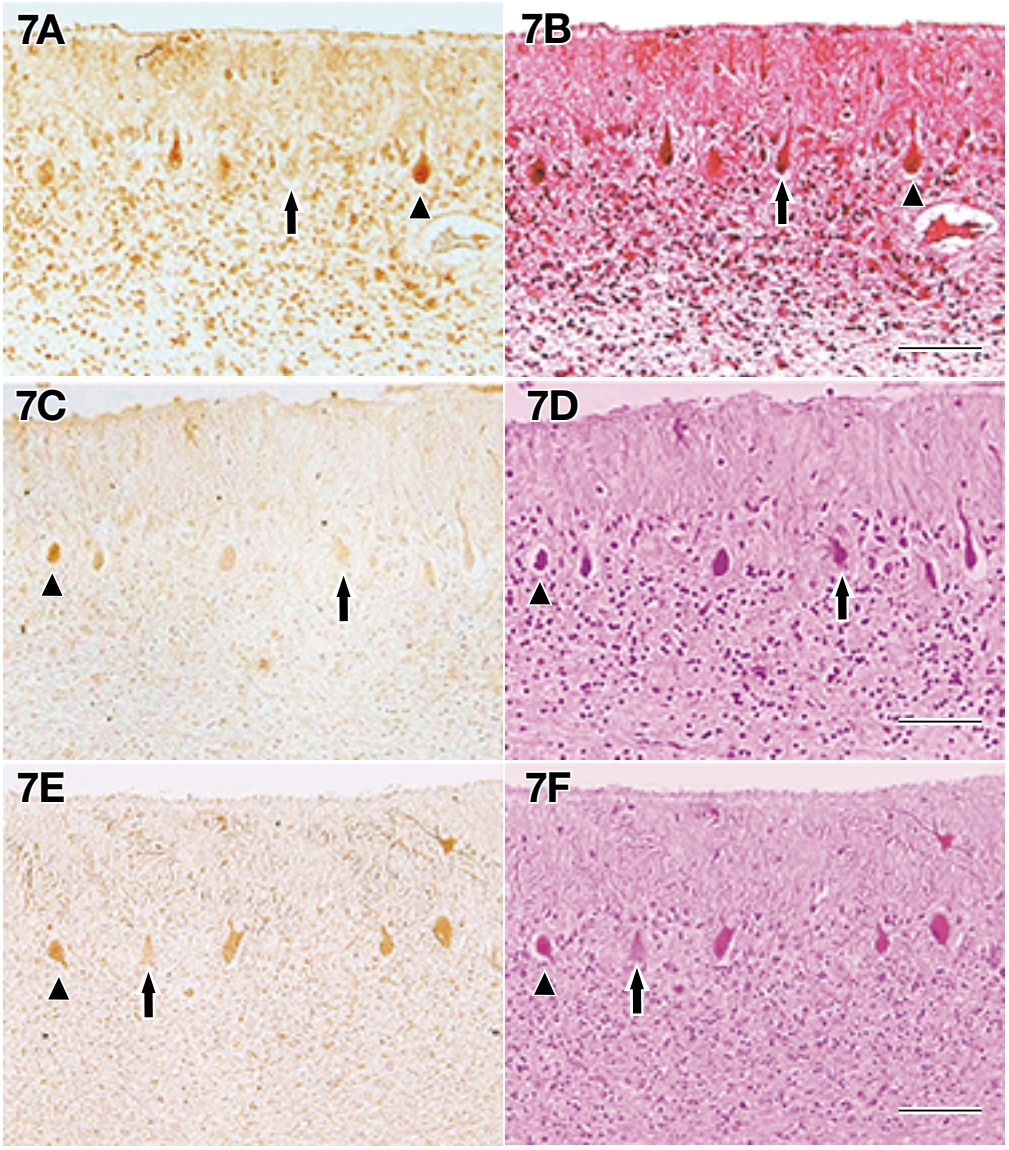

Fig. 7. Immunostaining of the cerebellum from a patient with MD using antibodies for HNE (**A**), acrolein (**C**) and hsp 32 (**E**).

A and **B:** Some of the remaining Purkinje cells (arrowhead in A and B) are positive for HNE, while other cells (arrow in **A** and **B**) are negative (**A:** HNE immunostaining without counterstaining. **B:** HE staining). Bar = 100 μm.

C and **D:** Some residual Purkinje cells are positive for acrolein (arrowhead in **C** and **D**), while other residual Purkinje cells are not (arrow in **C** and **D**) (**C:** acrolein immunostaining without counterstaining. **D:** HE staining). Bar = 100 μm.

E and **F:** Some of the remaining Purkinje cells (arrowhead in **E** and **F**) are immunoreactive for hsp 32, while other cells are not (arrow in **E** and **F**) (**E:** hsp 32 immunostaining without counterstaining. **F:** HE staining). Bar= 100 μm.

HNE, 4-hydroxy-2-nonenal; HE, hematoxylin and eosin; hsp, heat shock protein; MD, Menkes kinky hair disease.

patients were positive for acrolein. A variable staining intensity was observed (Fig. 7C), and the positive rate for anti-acrolein antibody was approximately 42% (420 ± 94.1/1,000) among the residual Purkinje cells. When acrolein-positive and acrolein-negative Purkinje cells were compared by HE staining, no marked differences between them were observed (Fig. 7D). Immunostaining with the anti-hsp 32 antibody showed that some of the residual Purkinje cells of MD patients were positive for hsp 32. There was variation of the staining intensity (Fig. 7E), and the positive rate for anti-hsp 32 antibody was approximately 40% (396 ± 73.5/1,000) among the residual MD Purkinje cells. When hsp 32-positive and hsp 32-negative Purkinje cells were compared by HE staining, there were no clear differences between them (Fig. 7F).

DISCUSSION

In the present neuropathological study of MD patients, marked loss of Purkinje cells and granule cells was ob-

served in the cerebellum. The residual Purkinje cells had the following neuropathological characteristics: somatic sprouts, cactus-like dendritic expansions, weeping willow extension of dendrites, heterotopia and axonal torpedoes.

Somatic sprouts are observed in Purkinje cells of the normal fetus around 27 weeks at autopsy.[4, 5] However, somatic sprouts are not observed in the normal fetus much past 27 weeks of gestation, so the sprouts disappear with increasing maturation.[4, 5] Thus, somatic sprouts are part of the normal developmental process, but should not be seen after birth. The fact that somatic sprouts were noted in all of the 7 MD autopsy cases (aged from 1 year and 1 month to 6 years and 4 months) suggests that the Purkinje cells of patients with MD have been affected by maldevelopment or developmental disorder.

Ectopic Purkinje cells were present in the granule cell layer of the cerebellum in MD autopsy cases, but not in the normal control autopsy cases. Purkinje cells originate from the neural tube and pass through the granule cell layer while migrating toward the Purkinje cell layer of the cerebellum.[30] Thus, normal migration results in Purkinje cells reaching the Purkinje cell layer, so the observation that MD patients have ectopic Purkinje cells suggests that these cells were arrested in the process of migrating toward the Purkinje cell layer and also indicates maldevelopment. Furthermore, based on the finding that ectopic Purkinje cells with somatic sprouts were present, cerebellar Purkinje cells in MD patients show evidence of maldevelopment.

The finding of weeping willow and cactus-like changes indicated abnormal enlargement of some dendrites. Dendritic expansion and cactus-like changes are assumed to arise during the process of dendrites extending from the Purkinje cell body. From this point of view, neuropathological findings such as dendritic expansion and cactus-like changes can be interpreted as further evidence of maldevelopment. On the other hand, it is also possible that after the Purkinje cell dendrites had developed fully, some dendrites underwent expansion and cactus-like changes due to degeneration. Thus, the neuropathology of dendritic expansion and cactus-like changes could be related to both maldevelopment and degeneration.

When development is normal, the dendrites of Purkinje cells extend from the cell bodies through the cerebellar molecular layer toward the side of the subarachnoid space. In contrast, the neuropathological weeping willow pattern is characterized by downwardly extending dendrites, and can be considered to arise from failure of the normal development of Purkinje cell dendrites. In this case, the weeping willow pattern is regarded as evidence of maldevelopment. On the other hand, the weeping willow pattern can also be interpreted as evidence of degeneration. There is a possibility that after the dendrites of Purkinje cells have fully developed, downward extension of some dendrites occurs as a result of shrinkage of their arborization. In other words, the weeping willow pattern could be regarded as due to maldevelopment and/or degeneration.

Axonal torpedoes of Purkinje cells like those in MD patients are frequently observed in autopsy cases of olivo-ponto-cerebellar atrophy, which is one of the neurodegenerative diseases.[31] Therefore, the axonal torpedoes seen in MD patients may be an indicator of degeneration.

Taken together, these findings indicate that cerebellar MD Purkinje cells undergo cell death due to both maldevelopment and degeneration. Comparison of the number of Purkinje cells in the 7 MD patients with that in the 39 normal controls revealed that almost half of the Purkinje cells had been lost in the MD patients. Thus, we clearly demonstrated that 50% of the Purkinje cells in MD patients died due to the effects of maldevelopment and degeneration.

There have been few reports about quantitative measurement of the number of Purkinje cells in the cerebellum. To the best of our knowledge, there is only one report by Hausmann et al.[32] concerning quantitative measurement of the number of Purkinje cells in normal autopsy cases. They studied 52 autopsy cases aged between 5 and 82 years and reported that the number of Purkinje cells per 1 mm length was 9.21 cells in 12 cases of sudden death and 7.60 cells in 18 cases of drowning or asphyxia that resulted in death within 10 min. In our study, the number of Purkinje cells was approximately 20.1 cells per 3 mm length in 39 normal control autopsy cases in the aged between 1 and 59 years. In the present study, patients exhibiting normal cerebellar histology who died because of organ failure and disorders outside the central nervous system were used as normal controls. None of them were cases of sudden deaths due to unknown etiology. When we assess the data of Hausmann et al. from this standpoint, our normal control group is similar to their 18 patients who died within 10 min due to drowning or asphyxia. Hausmann's data regarding the number of Purkinje cells could be converted to 22.8 cells per 3 mm length and this number is very close to our result for measurement of the number of Purkinje cells in the controls. Such concordance suggests the validity of the results of our quantitative analysis of the number of cerebellar Purkinje cells in normal controls and MD patients. In addition, we found that the number of Purkinje cells showed no significant difference among the age groups,

from the group less than 10 years old to the group in their 50s. Based on our data, the number of Purkinje cells in the normal cerebellum remains almost constant from 1 year to 59 years old.

Immunohistochemistry showed clear CCS staining from the cell bodies to the peripheral spiny branchlets of Purkinje cells. This immunohistochemical pattern suggests that CCS is an abundant protein in normal Purkinje cells. Similarly, SOD1 protein was abundant in normal Purkinje cells and was expressed from the cell body to the major dendrites. On the other hand, in MD patients with copper deficiency, the percentage of residual Purkinje cells positive for SOD1 was only about 23% and the intensity of staining was weak. In contrast, 77% of the remaining Purkinje cells were positive for CCS, which was higher than the rate for SOD1. In addition, the staining intensity for CCS was similar to that of normal control Purkinje cells. In other words, expression of CCS protein was maintained in MD Purkinje cells, but SOD1 protein was decreased.

There have been several reports about the levels of SOD1 and CCS protein in fresh tissues of copper-deficient animals. Bertinato et al.[33] fed one group of male Wistar rats a copper-deficient diet, while another group received a normal diet without copper deficiency, and they examined the levels of SOD1 and CCS protein in the liver and red blood cells of both groups by the western blotting method. SOD1 protein levels in both the liver and red blood cells were lower in the group receiving the copper-deficient diet compared with the group receiving a normal diet. In contrast, CCS protein levels were higher in both the liver and red blood cells of the group receiving the copper-deficient diet than in the group receiving a normal diet.[33] Prohaska et al.[34] used Holtzman rats and ND4 Swiss Webster mice to semi-quantitatively examine the levels of SOD1 and CCS protein in the liver and brain of copper-deficient diet groups and non-copper-deficient normal diet groups by western blot analysis. SOD1 protein levels were lower in the liver and brain of rats and mice from the copper-deficient groups than in those of rats and mice from the normal diet groups. SOD1 protein levels in the livers of rats and mice were 30% and 70%, respectively, while brain SOD1 protein levels were 83% and 22%, respectively. In contrast, CCS protein levels in the livers and brains of rats and mice from the copper-deficient diet groups were increased by approximately 3-fold in the rat liver, approximately 1.7-fold in the mouse liver, approximately 1.8-fold in the rat brain and approximately 2.8-fold in the mouse brain compared with the normal diet groups.[34] Furthermore, Gybina and Prohaska[35] compared cerebellar levels of CCS between Holtzman rats in the copper-deficient diet and normal diet groups. Compared with the CCS protein level in the normal diet group, the CCS protein level in the cerebellum of rats from the copper-deficient diet group was about 2-fold higher.[35]

In MD patients, Purkinje cells were exposed to copper deficiency for a very long period ranging from 1 year and 1 month to 6 years and 4 months, because MD is a copper absorption disorder. Copper deficiency is assumed to lead to a decrease of SOD1 protein, which is a copper-dependent enzyme. The duration of copper deficiency was only 42 days in the study of Bertinato,[33] 23 to 30 days in that of Prohaska[34] and 24 to 27 days in that of Gybiana.[35] Even with such short periods of copper deficiency, a decrease of SOD1 protein was observed in these animal experiments.[33–35] In our study, immunohistochemical staining showed that SOD1 expression was decreased in the residual Purkinje cells of MD patients. This reflected the fact that MD Purkinje cells had been subjected to severe damage caused by free radicals due to the chronic decrease of SOD1 activity. Under such circumstances, it would be difficult for the Purkinje cells of MD patients to maintain normal functions. On the other hand, while cell damage caused by free radicals secondary to the decrease of SOD1 could have occurred in the animal models of short-term copper deficiency, cell death was not observed.[33–35] This suggested that Purkinje cells were protected and survived as a result of up-regulating CCS, which specifically transports copper to SOD1. This up-regulation of CCS in the animals with short-term copper deficiency might correspond to the protective response of CCS in the remaining Purkinje cells of MD patients with chronic copper deficiency. According to our immunohistochemical results, even in the remaining Purkinje cells of MD patients that were close to the moribund state, CCS was maintained at almost the normal level. Based on this finding, the mechanism of CCS up-regulation still had a protective effect in the residual Purkinje cells of MD patients.

Our immunohistochemical analysis of HNE, acrolein and hsp 32 demonstrated that normal cerebellar Purkinje cells did not express any of HNE, acrolein or hsp 32. In the Purkinje cells of MD patients, however, we observed expression of HNE, acrolein and hsp 32 at varying intensities. The rate of positive staining for HNE, acrolein and hsp 32 in the remaining Purkinje cells of MD patients was 56%, 42% and 40%, respectively. HNE is a cytotoxic product that is generated when polyunsaturated fatty acids such as arachidonic acid are subjected to oxidative stress, and acrolein is another toxic metabolite generated when lipid membranes are subjected to oxidative stress. Therefore, immunohistochemical detection of both HNE and acrolein in the sur-

viving Purkinje cells of MD patients is strong evidence of oxidative stress. On the other hand, the immunohistochemical study also showed that hsp 32 was induced in the surviving Purkinje cells of MD patients. This could be regarded as evidence that hsp 32 was up-regulated in the surviving Purkinje cells as a self-protective mechanism against oxidative stress to promote survival. Kato et al.[4, 5] studied the expression of both hsp 27 and hsp 72 in the residual Purkinje cells of MD patients, and their results indicated that induction of both hsp 27 and hsp 72 occurs via a self-protective mechanism similar to that of hsp 32.[4, 5]

In conclusion, the present study demonstrated that i) in MD, approximately 50% of the Purkinje cells in the cerebellum die due to maldevelopment and degeneration. ii) In the residual Purkinje cells of patients with this disease, CCS expression is close to normal as a protective response to a decrease of SOD1 activity due to chronic copper deficiency. iii) In response to the increase of oxidative stress due to decreased SOD1 activity, hsp 32 is also induced as another protective mechanism.

Acknowledgments: The authors express their appreciation to Dr. K. Asayama for kindly providing the antibody to SOD1.

This study was supported in part by a Grant-in-Aid for Scientific Research (c) from the Ministry of Education, Culture, Sports, Science and Technology of Japan (S.K.: 24500420); a Grant-in Aid from the Scientific Committee of CNS Degenerative Diseases from the Ministry of Health, Labour and Welfare of Japan (S.K.); a Grant-in Aid for the physician training project in Shimane Prefecture (S.K.) and a Grant-in Aid for discretionary expenditure from the president of Tottori University (S.K.).

The authors declare no conflict of interest.

REFERENCES

1 Menkes JH, Alter M, Steigleder GK, Weakley DR, Sung JH. A sex-linked recessive disorder with retardation of growth, peculiar hair, and focal cerebral and cerebellar degeneration. Pediatrics. 1962;29:764-79. PMID: 14472668.

2 Aguilar MJ, Chadwick DL, Okuyama K, Kamoshita S. Kinky hair disease. I. Clinical and pathological features. J Neuropathol Exp Neurol. 1966;25:507-22. PMID: 5922550.

3 Danks DM, Campbell PE, Stevens BJ, Mayne V, Cartwright E. Menkes' kinky hair syndrome. An inherited defect in copper absorption with widespread effects. Pediatrics. 1972;50:188-201. PMID: 5045349.

4 Kato S, Ito M, Ohama E, Mikoshiba K, Maeda N, Yen SH, et al. Immunohistochemical studies on cerebellar Purkinje cells of Menkes' kinky hair disease. Neuropathology. 1993;13:159-66.

5 Kato S, Ito M, Ohama E, Mikoshiba K, Maeda N, Hirano A. Immunohistochemical investigation on cerebellar Purkinje cells of Menkes' kinky hair disease: disappearance of inositol 1,4,5-triphosphate receptor protein, and expression of phosphorylated neurofilament proteins, αB-crystallin and stress-response proteins. Neuropathology. 1993;13:305-9.

6 Becker LE, Yates AJ. Metabolic disease. In: Davis RL, Robertson DM, editors. Textbook of Neuropathology, 3rd ed. Baltimore: Williams & Wilkins; 1997. p. 407-91.

7 Ince PG, Wharton SB. Disease of movement and system degenerations. In: Love S, Louis DN, Ellison DW, editors. Greenfield's Neuropathology, 8th ed. London: Edward Arnold; 2008. p. 889-981.

8 Ghatak NR, Hirano A, Poon TP, French HJ. Trichopoliodystrophy. II. Pathological changes in skeletal muscle and nervous system. Arch Neurol. 1972;26:60-72. PMID: 4108802.

9 Purpura DP, Hirano A, French JH. Polydendritic Purkinje cells in X-chromosome linked copper malabsorption: a Golgi study. Brain Res. 1976;117:125-9. PMID: 990927.

10 Troost D, van Rossum A, Straks W, Willemse J. Menkes' kinky hair disease. II. A clinicopathological report of three cases. Brain Dev. 1982;4:115-26. PMID: 7091568.

11 Shibata N, Hirano A, Kobayashi M, Umahara T, Kawanami T, Asayama K. Cerebellar superoxide dismutase expression in Menkes' kinky hair disease: an immunohistochemical investigation. Acta Neuropathol. 1995;90:198-202. PMID: 7484097.

12 Takikawa M, Kato S, Esumi H, Kurashima Y, Hirano A, Asayama K, et al. Temprospatial relationship between the expressions of superoxide dismutase and nitric oxide synthase in the developing human brain: immunohistochemical and immunoblotting analyses. Acta Neuropathol. 2001;102:572-8. PMID: 11761717.

13 Fridovich I. Superoxide dismutases. Adv Enzymol Relat Areas Mol Biol. 1986;58:61-97. PMID: 3521218.

14 Kato S, Kato M, Abe Y, Matsumura T, Nishino T, Aoki M, et al. Redox system expression in the motor neurons in amyotrophic lateral sclerosis (ALS): immunohistochemical studies on sporadic ALS, superoxide dismutase 1 (SOD1)-mutated familial ALS, and SOD1-mutated ALS animal models. Acta Neuropathol. 2005;110:101-12. PMID: 15983830.

15 Kato S, Saeki Y, Aoki M, Nagai M, Ishigaki A, Itoyama Y, et al. Histological evidence of redox system breakdown caused by superoxide dismutase 1 (SOD1) aggregation is common to SOD1-mutated motor neurons in humans and animal models. Acta Neuropathol. 2004;107:149-58. PMID: 14648077.

16 Culotta VC, Klomp LW, Strain J, Casareno RL, Krems B, Gitlin JD. The copper chaperone for superoxide dismutase. J Biol Chem. 1997;272:23469-72. PMID: 9295978.

17 Rothstein JD, Dykes-Hoberg M, Corson LB, Becker M, Cleveland DW, Price DL, et al. The copper chaperon CCS is abundant in neurons and astrocytes in human and rodent brain. J Neurochem. 1999;72:422-9. PMID: 9886096.

18 Casareno RL, Waggoner D, Gitlin JD. The copper chaperone CCS directly interacts with cupper/zinc superoxide dismutase. J Biol Chem. 1998;273:23625-8. PMID: 9726962.

19 Rae TD, Schmidt PJ, Pufahl RA, Culotta VC, O'Halloran TV. Undetectable intracellular free copper: the requirement of a copper chaperone for superoxide dismutase. Science. 1999;284:805-8. PMID: 10221913.

20 Wong PC, Waggoner D, Subramaniam JR, Tessarollo L, Bartnikas TB, Culotta VC, et al. Copper chaperone for superoxide dismutase is essential to activate mammalian Cu/Zn superoxide dismutase. Proc Natl Acad Sci USA. 2000;97:2886-91. PMID: 10694572.

21 Peña MM, Lee J, Thiele DJ. A delicate balance: homeostatic control of copper uptake and distribution. J Nutr. 1999;129:1251-60. PMID: 10395584.

22 Petris MJ, Smith K, Lee J, Thiele DJ. Copper-stimulated endocytosis and degradation of the human copper transporter,

hCtr1. J Biol Chem. 2003;278:9639-46. PMID: 12501239.
23 Kato S, Sumi-Akamaru H, Fujimura H, Sakoda S, Kato M, Hirano A, et al. Copper chaperone for superoxide dismutase co-aggregates with superoxide dismutase 1 (SOD1) in neuronal Lewy body-like hyaline inclusions: an immunohistochemical study of familial amyotrophic lateral sclerosis with SOD1 gene mutation. Acta Neuropathol. 2001;102:233-8. PMID: 11585247.
24 Sumi-Akamaru H, Fujimura H, Kato S, Takayasu S, Eto M, Ohama E, et al. Immunohistochemical analysis of copper chaperone for superoxide dismutase in mouse central nervous system: a comparative study with paraffin and frozen section. Acta Histochem Cytochem. 2002;35:33-8.
25 Kato S, Horiuchi S, Liu J, Cleveland DW, Shibata N, Nakashima K, et al. Advanced glycation endproducto-modified superoxide disumutase-1 (SOD1)-positive inclusions are common to familial amyotrophic lateral sclerosis patients with SOD1 gene mutations and transgenic mice expressing human SOD1 with a G85R mutation. Acta Neuropathol. 2000;100:490-505. PMID: 11045671.
26 Kato S, Esumi H, Hirano A, Kato M, Asayama K, Ohama E. Immunohistochemical expression of inducible nitric oxide synthase (iNOS) in human brain tumors: relationships of iNOS to superoxide dismutase (SOD) proteins (SOD1 and SOD2), Ki-67 antigen (MIB-1) and p53 protein. Acta Neuropathol. 2003;105:333-40. PMID: 12624786.
27 Kato S, Shimoda M, Watanabe Y, Nakashima K, Takahashi K, Ohama E. Familial amyotrophic lateral sclerosis with a two base pair deletion in superoxide dismutase 1: gene multisystem degeneration with intracytoplasmic hyaline inclusions in astrocytes. J Neuropathol Exp Neurol. 1996;55:1089-101. PMID: 8858006.
28 Kato S, Hayashi H, Nakashima K, Nanba E, Kato M, Hirano A, et al. Pathological characterization of astrocytic hyaline inclusions in familial amyotrophic lateral sclerosis. Am J Pathol. 1997;151:611-20. PMID: 9273821.
29 Kato S, Horiuchi S, Nakashima K, Hirano A, Shibata N, Nakano I, et al. Astrocytic hyaline inclusions contain advanced glycation endproducts in familial amyotrophic lateral sclerosis with superoxide dismutase 1 gene mutation: immunohistochemical and immunoelectron microscopical analyses. Acta Neuropathol. 1999;97:260-6. PMID: 10090673.
30 Friede RL. Gross and microscopic development of central nervous system. In: Friede RL, editor. Developmental neuropathology, 2nd ed. Berlin: Springer-Verlag; 1989. p.12-6.
31 Kato S, Hayashi H, Mikoshiba K, Hirano A, Yen SH, Ohama E. Purkinje cells in olivopontocerebellar atrophy and granule cell-type cerebellar degeneration: an immunohistochemical study. Acta Neuropathol. 1998;96201:67-74. PMID: 9678515.
32 Hausmann R, Seidl S, Betz P. Hypoxic changes in Purkinje cells of the human cerebellum. Int J Legal Med. 2007;121:175-83. PMID: 17031692.
33 Bertinato J, Iskandar M, L'Abbé MR. Copper deficiency induces the upregulation of the copper chaperone for Cu/Zn superoxide dismutase in weanling male rats. J Nutr. 2003;133:28-31. PMID: 12514262.
34 Prohaska JR, Broderius M, Brokate B. Metallochaperone for Cu,Zn-superoxide dismutase (CCS) protein but not mRNA is higher in organs from copper-deficient mice and rats. Arch Biochem Biophys. 2003;417:227-34. PMID: 12941305.
35 Gybina AA, Prohaska JR. Variable response of selected cuproproteins in rat choroid plexus and cerebellum following perinatal copper deficiency. Genes Nutr. 2006;1:51-9. PMID: 18850220.
36 Iwata M, Hirano A, French JH. Thalamic degeneration in X-chromosome-linked copper malabsorption. Ann Neurol. 1979;5:359-66. PMID: 443770.
37 Iwata M, Hirano A, French JH. Degeneration of the cerebellar system in X-chromosome-linked copper malabsorption. Ann Neurol. 1979;5:542-9. PMID: 475349.
38 Inagaki M, Hashimoto K, Yoshino K, Ohtani K, Nonaka I, Arima M, et al. Atypical form of Menkes kinky hair disease with mitochondrial NADH-CoQ reductase deficiency. Neuropediatrics. 1988;19:52-5. PMID: 2452375.